

VIP Very Important Paper

# Interrogating PP1 Activity in the MAPK Pathway with Optimized PP1-Disrupting Peptides

Yansong Wang,<sup>[a]</sup> Bernhard Hoermann,<sup>[a, b, c]</sup> Karolina Pavic,<sup>[a]</sup> Malgorzata Trebacz,<sup>[b]</sup> Pablo Rios,<sup>[b]</sup> and Maja Köhn<sup>\*[a, b]</sup>

Protein phosphatase-1 (PP1)-disrupting peptides (PDPs) are selective chemical modulators of PP1 that liberate the active PP1 catalytic subunit from regulatory proteins; thus allowing the dephosphorylation of nearby substrates. We have optimized the original cell-active PDP3 for enhanced stability, and obtained insights into the chemical requirements for stabilizing this 23-mer peptide for cellular applications. The optimized PDP-Nal was used to dissect the involvement of PP1 in the MAPK signaling cascade. Specifically, we have demonstrated that, in human osteosarcoma (U2OS) cells, phosphoMEK1/2 is a direct substrate of PP1, whereas dephosphorylation of phosphoERK1/2 is indirect and likely mediated through enhanced tyrosine phosphatase activity after PDP-mediated PP1 activation. Thus, as liberators of PP1 activity, PDPs represent a valuable tool for identifying the substrates of PP1 and understanding its role in diverse signaling cascades.

Protein phosphatase-1 (PP1) is a Ser/Thr-specific phosphoprotein phosphatase (PPP) that has central roles in cellular and organismal physiology, and has been implicated in several human diseases associated with deregulated phosphorylation.<sup>[1–3]</sup> PP1 holoenzymes each contain a conserved catalytic subunit with an active-site pocket that is highly similar to that of other PPPs, and one or two regulatory proteins that determine substrate specificity, cellular localization, or activity.<sup>[2]</sup> A major obstacle to understanding the roles of PP1 in cellular signaling pathways is the lack of tools to selectively modulate PP1 activity without influencing other PPPs.<sup>[4,5]</sup> To address this

need for selective chemical modulators for PP1, we previously developed PP1-disrupting peptides (PDPs).<sup>[6]</sup> PDPs liberate the catalytic subunit of PP1 from the holoenzyme, thereby generating a cellular pool of active PP1 inside the cell that can dephosphorylate nearby substrates.<sup>[6]</sup> PDPs are selective towards PP1 over related phosphatases, and thus, represent valuable tools to study PP1 function in physiological and pathological processes.<sup>[3,6,7]</sup> Notably, recently it was shown that PDP treatment of human heart failure patient samples led to PP1 counteracting increased kinase activity and successfully sealing the arrhythmogenic Ca<sup>2+</sup> leak.<sup>[3a]</sup> In these studies, the cell-active PDP3 was applied; this contained the unnatural amino acid *para*-benzoylphenylalanine (*Bpa*), which imparts metabolic stability to the PDP (Table 1). If L-alanine were used in place of the *Bpa*, the peptide, called PDP2, was cell penetrating, but

**Table 1.** PDPs used for this study and their EC<sub>50</sub> values for de-inhibiting PP1 (25 μM) by disrupting its interaction with inhibitor-2 (I2; 1 nM) and using DiFMUP (135 μM) as a substrate. All peptides were acetylated at the N terminus and amidated at the C terminus. The variable position in the sequence is marked in italics. PDPm: inactive mutant.<sup>[6]</sup> Related graphs are found in Figure S1 in the Supporting Information. The results are presented as the mean ± standard error of the mean (n = 3).

| Peptide  | Sequence  | EC <sub>50</sub> [nM] |
|----------|---|-----------------------|
| PDP3     | RRKRPKRKRKNARVTF <i>Bpa</i> EAAEII <sup>[a]</sup> | 380 ± 19              |
| PDP-βal  | RRKRPKRKRKNARVTFβalEAAEII <sup>[b]</sup>          | 49 ± 8                |
| PDP-dal  | RRKRPKRKRKNARVTFdalEAAEII <sup>[c]</sup>          | 343 ± 45              |
| PDP-Nal  | RRKRPKRKRKNARVTFNalEAAEII <sup>[d]</sup>          | 144 ± 40              |
| PDPm-Nal | RRKRPKRKRKNARATANalEAAEII                         | inactive              |

[a]

*para*-benzoylphenylalanine (*Bpa*)

[b]

β-alanine (βal)

[c]

D-alanine (Dal)

[d]

2-naphthylalanine (Nal)

[a] Dr. Y. Wang, B. Hoermann, Dr. K. Pavic, Prof. Dr. M. Köhn  
Genome Biology Unit  
European Molecular Biology Laboratory  
Meyerhofstrasse 1, 69117 Heidelberg (Germany)

[b] B. Hoermann, M. Trebacz, Dr. P. Rios, Prof. Dr. M. Köhn  
Faculty of Biology and BIOS-Centre for Biological Signalling Studies  
Albert-Ludwigs-University of Freiburg  
Schänzlestrasse 18, 79104 Freiburg (Germany)  
E-mail: maja.koehn@bioss.uni-freiburg.de

[c] B. Hoermann  
Collaboration for joint PhD degree between EMBL and  
Heidelberg University, Faculty of Biosciences  
Heidelberg (Germany)

Supporting information and the ORCID identification numbers for the authors of this article can be found under <https://doi.org/10.1002/cbic.201800541>.

© 2018 The Authors. Published by Wiley-VCH Verlag GmbH & Co. KGaA. This is an open access article under the terms of the Creative Commons Attribution Non-Commercial NoDerivs License, which permits use and distribution in any medium, provided the original work is properly cited, the use is non-commercial and no modifications or adaptations are made.

not stable, and therefore not active in releasing PP1 to dephosphorylate histone H3 on phosphothreonine 3 (H3pThr3) in cells.<sup>[6]</sup> However, the photolability of *Bpa* makes the handling of PDP3 cumbersome. Therefore, we set out to optimize PDP3 to circumvent photolability, but preserve stability, and to understand which chemical features of *Bpa* conferred cellular stability to PDPs. In addition, to evaluate the performance of

the optimized PDP relative to that of PDP3, we chose to interrogate the influence of PP1 activity on the mitogen-activated protein kinase (MAPK)/extracellular-signal activated kinase (ERK) pathway. This signaling pathway has central roles in cell growth and differentiation, and in cancer development and progression. It involves a cascade of three key protein kinases—rapidly accelerated fibrosarcoma (Raf), MAPK/ERK kinase (MEK), and ERK—that successively phosphorylate and activate one another.<sup>[6]</sup> PP1 regulates MAPK/ERK signaling at several levels. Raf1 is a direct substrate of PP1.<sup>[9–13]</sup> For MEK and ERK, however, the role of PP1 is less clear and is likely to be context-dependent, leading to different conclusions as to whether they are direct substrates or not.<sup>[9,14–18]</sup> Critical issues are the dependence of the phosphorylation levels of MEK and ERK on upstream kinase activity, signal amplification in the cascade, and the presence of feedback loops.<sup>[6]</sup> This makes it difficult to distinguish direct dephosphorylation from reduced phosphorylation through reduced upstream kinase activity in cellular experiments. Thus, we aimed to address herein whether PDPs, which trigger PP1 activity in an acute and specific manner, could be used to clarify such relationships in signaling cascades, by using the MAPK/ERK cascade as an example.

To determine whether it is the bulkiness of *Bpa* or the fact that it is an unnatural amino acid that accounts for the cellular stability it imparts to PDP3, we synthesized PDPs that contained the small amino acids *D*-alanine (*Dal*),  $\beta$ -alanine ( *$\beta$ al*), or bulky 2-naphthylalanine (*Nal*). First, we tested if these PDPs disrupted in vitro the interaction of PP1 with the regulatory protein I2 to liberate PP1, such that it could dephosphorylate the fluorogenic substrate 6,8-difluoro-4-methylumbelliferyl phosphate (DiFMUP).<sup>[6,19]</sup> The results show that all peptides maintain in vitro activity in a similar potency range, with PDP3 showing the highest EC<sub>50</sub> (Table 1 and Figure S1 in the Supporting Information).

Next, we tested the cellular stability of these peptides in U2OS human osteosarcoma cells.<sup>[6]</sup> The cells were incubated with 10  $\mu$ M 5-carboxyfluorescein (FAM)-labeled peptides for 3 h at 37 °C, washed thoroughly, and lysed to determine the remaining amount of intact peptides in the cells by fluorescence in-gel scanning.<sup>[6]</sup> FAM-PDP3 and FAM-PDP-*Nal* were similarly stable and significantly more stable than that of FAM-PDP- $\beta$ al and FAM-PDP-*dal*, which were almost completely degraded (Figure 1A). After 30 min, residual levels of the last two peptides were still visible (Figure S2). Because the cell-penetration properties of the PDPs are generally not altered through modifications at this position in the peptide,<sup>[6]</sup> these findings suggest that the bulky residue is required for the observed cellular stability of PDPs.

We then analyzed the photostability of PDP-*Nal*, relative to that of PDP3. To this end, we irradiated the peptides with UV light ( $\lambda = 365$  nm) for 5 min or kept them at room temperature under ambient light for 24 h. The HPLC traces of the peptides after these treatments show that PDP-*Nal* has a much greater photostability than that of PDP3 (Figure 1B and Figure S3).

Subsequently, we evaluated the activity of PDP-*Nal* in cells. Phosphorylated histone H3 (pThr3) is a marker of mitosis and a well-established substrate of PP1.<sup>[20]</sup> Therefore, we evaluated

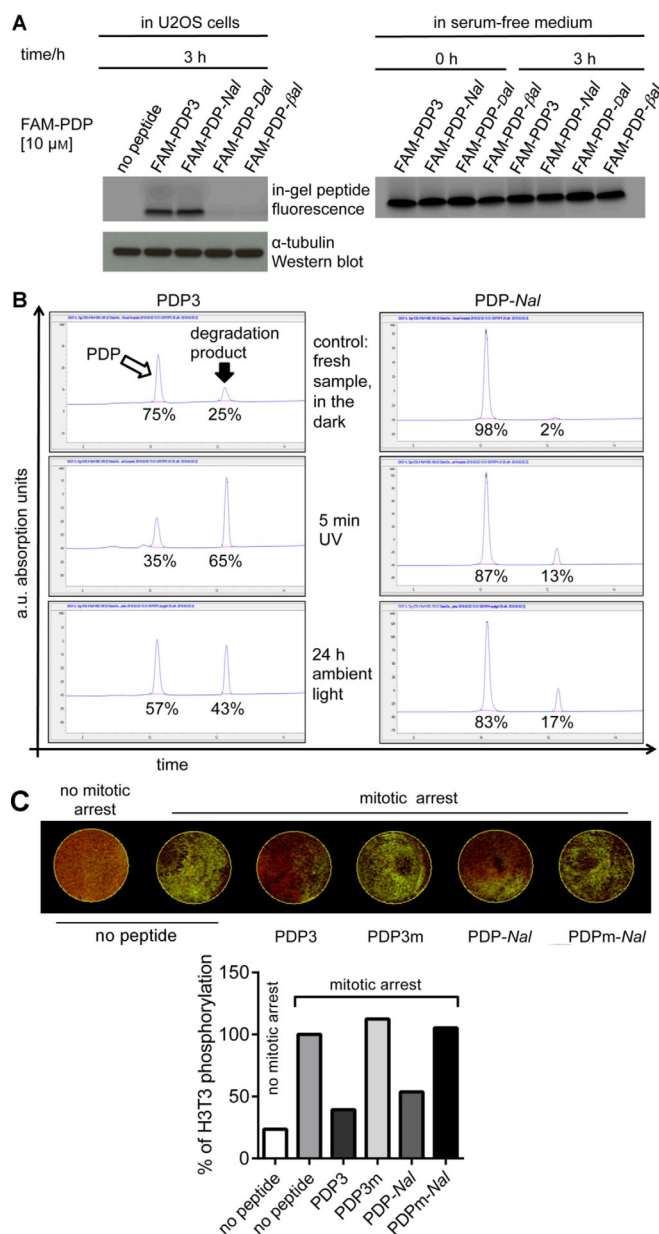


**Figure 1.** PDP-*Nal* is an optimized version of PDP3. A) Fluorescence gels of the peptides (10  $\mu$ M) from total U2OS cell lysate and SFM, showing in-cell stability after incubation for the indicated time points. An immunoblotting for  $\alpha$ -tubulin serves as a loading control. B) HPLC traces (gradient 10–90% acetonitrile) measured at  $\lambda = 230$  nm absorption for PDP3 and PDP-*Nal* after the indicated treatments. Illumination with UV light for 5 min at  $\lambda = 365$  nm or storage 24 h under daylight. Control: no light treatment; sample was freshly prepared and kept in the dark. Percentages indicate the relative area below the respective peak. Full spectra are shown in Figure S3. Results are representative of two experiments. C) Histone H3pThr3 dephosphorylation by PDP3 and PDP-*Nal* in U2OS cells. Immunofluorescence analysis after incubation for 30 min with 40  $\mu$ M of the respective peptides (green: histone H3pThr3; red: histone H3; well diameter: 22.2 mm) and the respective quantification of the signal intensity of H3pThr3/H3T3 relative to that from “mitotic arrest, no peptide,” which was set to 100%. Results are representative of three experiments.

the ability of PDP-*Nal* to promote dephosphorylation of histone H3pThr3 in cells, as previously shown for PDP3.<sup>[6]</sup> U2OS cells were arrested in mitosis and incubated with the peptides.

The cells were washed and stained with fluorescent antibodies against total histone H3 and histone H3pThr3. Similar to PDP3, PDP-*Nal* caused marked dephosphorylation of H3pThr3 (Figure 1C). As expected, the inactive variants of the PDPs—PDP3m and PDPm-*Nal*—failed to trigger dephosphorylation of histone H3. Thus, optimized PDP-*Nal* shows increased photostability and higher in vitro potency than that of PDP3, while retaining cellular penetration and stability.

In the following, we wanted to evaluate the performance of PDP3 and PDP-*Nal* in interrogating the MAPK pathway for PP1 activity. From data reported in the literature, it was unclear if PP1 could dephosphorylate pMEK1/2 and pERK1/2 directly, so we first sought to address this issue in U2OS cell lysates, in which MAPK signaling is constitutively active.<sup>[21]</sup> To this end, we disrupted signaling by pretreating the cells with the phosphatase inhibitor calyculin A (CalA) and Na<sub>3</sub>VO<sub>4</sub>, to inhibit endogenous phosphatases, which was followed by cell lysis. Subsequently, recombinant PP1 or mock control was added. In this assay, we saw clear dephosphorylation of pMEK1/2 (Ser217/Ser221) and pRaf1 (Ser259), which is a known substrate of PP1,<sup>[13]</sup> and therefore served as a control (Figure 2A). However, we did not observe dephosphorylation of pERK1/2 (Thr202/Tyr204) under these conditions. To clarify whether pMEK1 (Ser217/Ser221) and pERK1 (Thr202) were substrates of PP1, we incubated overexpressed, immunoprecipitated GFP-MEK1 and FLAG-ERK1 with recombinant PP1. At high PP1 concentrations (125 nM), at which dephosphorylation activity would reportedly be visible,<sup>[1,15]</sup> pMEK1 was completely dephosphorylated, whereas no change in pERK1 was observed; this confirmed that pERK1 (Thr202) was not a direct substrate of PP1 under

these conditions (Figure 2B). On the other hand, direct dephosphorylation of pMEK1 was dependent on the concentration of PP1 and could be inhibited by treatment with CalA; thus confirming pMEK1 as a PP1 substrate.

We next asked whether we could apply the PDPs in intact cells to distinguish the observed different activity of PP1 on pMEK1/2 and pERK1/2. Cells were treated with the peptides for different lengths of time, then lysed and analyzed by means of western blot for the phosphorylation status of pMEK1/2 (Ser217/221) and pERK1/2 (Thr202/Tyr204). Relative to cells not treated with peptides, cells treated for 20 min or longer with PDP3 or PDP-*Nal* showed decreased levels of phosphorylation of pMEK1/2 and pERK1/2 (Figure 3A). The peptides had the strongest effect on pERK1/2. Although this result is in agreement with previous observations of elevated phosphorylation levels upon PP1 knockdown or upon inhibition of phosphatases with CalA, okadaic acid, and tautomycin,<sup>[9,16]</sup> it contradicted our in vitro experiments. To address this, we considered the potential action of other phosphatases downstream of PDP-liberated PP1. ERK1/2 is a known target of dual specificity phosphatases (DUSPs) of the protein tyrosine phosphatase (PTP) superfamily, which are prone to deactivation by oxidation of their catalytically active cysteine.<sup>[22]</sup> Furthermore, Na<sub>3</sub>VO<sub>4</sub> is a general inhibitor of PTPs. Combined H<sub>2</sub>O<sub>2</sub>/Na<sub>3</sub>VO<sub>4</sub> pretreatment leads to full inhibition of PTPs, and, if followed by PDP treatment, would allow comparison of the influence of PTPs and PP1 on the dephosphorylation of pMEK1/2 and pERK1/2. Although pMEK1/2 was still dephosphorylated upon pretreatment with H<sub>2</sub>O<sub>2</sub>/Na<sub>3</sub>VO<sub>4</sub>, together with PDP addition, PDP-induced pERK1/2 dephosphorylation was markedly impaired in

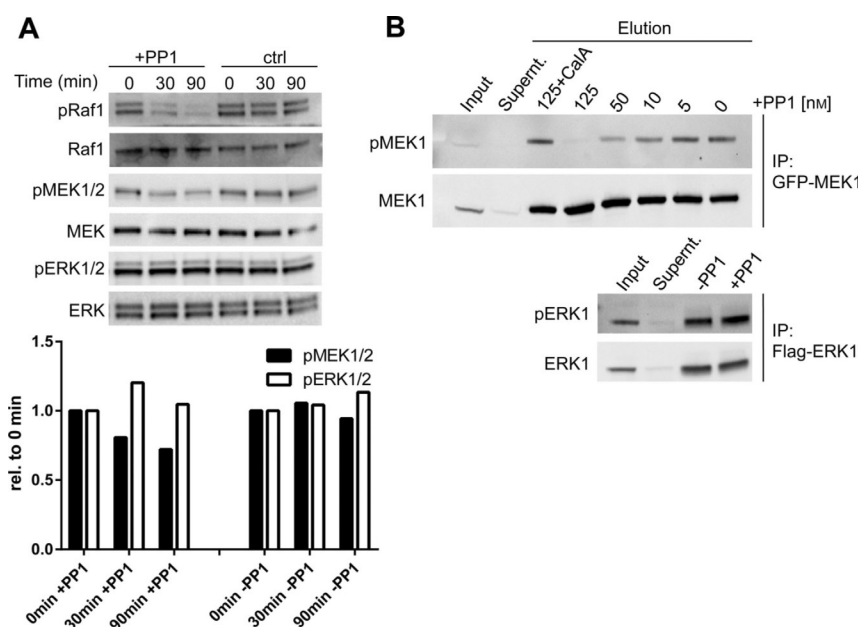


**Figure 2.** Interrogating the activity of recombinant PP1 towards MAPKs. A) Dephosphorylation of MAPKs in U2OS cell lysates by using recombinant PP1 (1  $\mu$ M). Cell lysates were analyzed by means of western blot for Raf1, MEK1/2, and ERK1/2, and for the phosphorylated forms of these proteins (pRaf1 (Ser259), pMEK1/2 (Ser217/Ser221), pERK1/2 (Thr202/Tyr204)). Shown below is the respective quantification relative to the signal intensity of "0 min + PP1," which was set to 1.0. Results are representative of three experiments. B) Dephosphorylation of purified MAPKs by PP1. Overexpressed GFP-MEK1 and FLAG-ERK1 were immunoprecipitated, and subsequently treated with different concentrations of recombinant PP1. Protein reactions were analyzed by western blot for MEK1/2, ERK1/2, pMEK1/2 (Ser217/Ser221), and pERK1/2 (Thr202). Results are representative of three experiments.

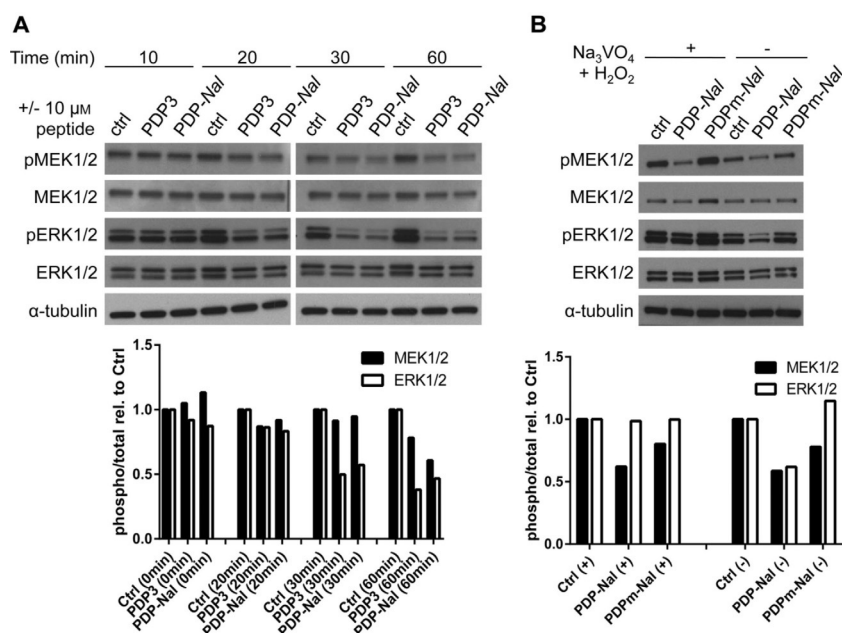


**Figure 3.** Interrogating endogenous PP1 activity towards MAPKs in cells by using PDPs. A) MAPK signaling in U2OS cells left untreated (ctrl) or treated for the indicated lengths of time with PDP-Nal or PDP3. Cells were analyzed by western blot for MEK1/2, ERK1/2, pMEK1/2 (Ser217/Ser221), and pERK1/2 (Thr202/Thr204). Shown below is the respective quantification for the signal intensities of pMEK/MEK and pERK/ERK; all relative to "Ctrl (0 min)," which was set to 1.0. Results are representative of two experiments. B) Effect of the inhibition of tyrosine phosphatases ( $\text{H}_2\text{O}_2/\text{Na}_3\text{VO}_4$  treatment, 30 min) on MAPK signaling 30 min after treatment with 10  $\mu\text{M}$  PDP-Nal and PDPm-Nal. Analysis as in A). Shown below is the respective quantification, which has been normalized as in (A). Results are representative of two experiments.

the presence of  $\text{H}_2\text{O}_2/\text{Na}_3\text{VO}_4$  (Figure 3B for PDP-Nal and Figure S4 for PDP3). This suggests that pERK1/2 is dephosphorylated by DUSPs/PTPs downstream of PDP-liberated PP1, whereas the dephosphorylation of pMEK1/2 did not depend on these phosphatases. As expected, the PDPm negative controls did not significantly influence the phosphorylation status of pMEK or pERK (Figure 3B for PDPm-Nal and Figure S4 for PDP3m).

In summary, we have described herein the optimization of PDP3 for photostable PDP-Nal. Analysis of PDP3 variants revealed that the bulkiness of the residue at position 17 was required for cellular stability. We showed that PDP-Nal could be applied in combination with other chemical modulators to help with dissecting the involvement of PP1 in signaling pathways by using the MAPK pathway as an example. Specifically, our data suggest that pMEK1/2 is a direct substrate of PP1, whereas pERK1/2 is not directly dephosphorylated by PP1 in U2OS cells, but rather by DUSPs/PTPs that act downstream of the PDP-liberated PP1.

## Experimental Section

Peptide synthesis and labeling procedures, sources of reagents and recombinant proteins, cell cultures, and SDS page and Western blotting procedures are described in the Supporting Information.

**In vitro phosphatase activity assay:** Recombinant PP1 protein (25  $\mu\text{M}$  final assaying concentration), 12 phosphatase inhibitor (1 nM final assaying concentration), and PDP at various concentrations were incubated in assay buffer (25 mM imidazole, 50 mM NaCl, bovine serum albumin (BSA; 0.1 mg mL<sup>-1</sup>), 1 mM dithiothrei-

tol (DTT), 0.3 mM  $\text{MnCl}_2$ , pH 7.4) for approximately 20 min at 25 °C followed by addition DiFMUP to reach a final concentration of 135  $\mu\text{M}$  ( $K_m$  value). The dephosphorylation of DiFMUP to the fluorescent product was monitored for 20 min on a TECAN Infinite M1000 PRO fluorescence microplate reader with excitation at  $\lambda = 358$  nm and emission at  $\lambda = 452$  nm. All experiments were performed in triplicate. After baseline normalization (assay in the absence of PDP), the reaction rates were plotted versus the log of the inhibitor concentrations, and the  $\text{EC}_{50}$  values were obtained by fitting the curves by using the one-site competition model of GraphPad Prism (GraphPad Software, version 5). The  $K_m$  value of DiFMUP for PP1 was determined by measuring the reaction kinetics of a substrate dilution series. Initial velocities were plotted against DiFMUP concentration, and the data was analyzed by Michaelis–Menten kinetics curve fitting in GraphPad Prism.

**Cellular stability of the peptides:** Dishes with a diameter of 3.5 cm containing equal numbers of U2OS cells were treated with 10  $\mu\text{M}$  fluorescently labeled (FAM) PDPs. After 3 h, the cells were washed three times with warm phosphate-buffered saline (PBS), scraped, pelleted, and total lysates were prepared by boiling with SDS sample buffer. The same volume of the total lysates from different conditions was run on a 12% Bis-Tris gel by using 2-(*N*-morpholino)ethanesulfonic acid (MES) running buffer. The fluorescent bands of the peptides were visualized by using a fluorescent imager (FLA-7000; FujiFilm) and corresponded to their expected size. After imaging, the proteins on the SDS gel were transferred onto a nitrocellulose membrane and subjected to western blotting against  $\alpha$ -tubulin as a loading control. The images were analyzed and quantified by using ImageJ 1.49m software (National Institutes of Health).

**UV stability of the peptides:** PDPs were diluted in PBS at a final concentration of 20  $\mu\text{M}$ . Samples were either exposed to UV light

(120 micro Joules per  $\text{cm}^2$ ) for 5 min, by using a UVP crosslinker 365 nm CL-1000L ( $\lambda = 365$  nm) instrument, or kept in ambient light for 24 h at RT. Samples were then analyzed by means of HPLC (Agilent) with a gradient of 10–90%  $\text{H}_2\text{O}/\text{CH}_3\text{CN}$  over 25 min.

**Histone H3 dephosphorylation assay and in-cell western blot:** Equal numbers of U2OS cells were cultured in 12-well plates (Greiner Bio-One CELLSTAR). To arrest mitosis, cells were treated with thymidine for 24 h, then 2 h without thymidine, and 14 h with nocodazole. PDPs (40  $\mu\text{M}$ ) were subsequently added to the nocodazole-containing media. After 30 min of peptide treatment, the cells were fixed with ice-cold methanol for 10 min with gentle shaking, and then washed with PBS. Odyssey Blocking Buffer (LI-COR) was used for blocking (1.5 h) and antibody dilutions. Samples were incubated for 2 h at RT with a 1:500 dilution of primary antibodies against phosphohistone H3 (Thr3; Millipore; cat. no. 07-424) and total histone H3 hosted (Active Motif; cat. no. 39763) antibodies. Cells were washed three times for 5 min with 0.5% Triton X-100 in PBS and then incubated for 1 h in a 1:1000 dilution of secondary IRDye 800CW goat anti-rabbit IgG (H+L) (LI-COR, cat. no. 925-32211) and IRDye 680RD goat anti-mouse IgG (H+L) (LI-COR, cat. no. 925-68070). After three 5 min washes with 0.5% Triton X-100 in PBS, PBS (500  $\mu\text{L}$ ) was added to each well and images of the plates were acquired on a LI-COR Odyssey CLx Imager.

**Dephosphorylation assay in cell lysates:** U2OS cells were cultivated in growth medium on 10 cm cell culture dishes (Nunc, Thermo Scientific). After reaching 90% confluency, cells were washed with PBS and incubated in serum-free medium (SFM) containing 1 mM  $\text{Na}_3\text{VO}_4$ , 0.33 mM  $\text{H}_2\text{O}_2$ , and 20  $\mu\text{M}$  Cal A PP1/PP2A inhibitor (Merck Millipore) for 20 min at 37 °C. The cells were then washed twice with cold PBS and scraped in lysis buffer (1 mL; 10 mM Tris-HCl, 137 mM NaCl, 10% glycerol, 1% NP-40, 20 mM CalA, 1 mM  $\text{Na}_3\text{VO}_4$ , 1  $\times$  PIC). The lysate was incubated on ice for 10 min and then cleared by centrifugation. The cleared lysate was then used to set up the individual 100  $\mu\text{L}$  reactions of the dephosphorylation assay. To this end, lysate was mixed with indicated amounts of recombinant PP1 $\alpha$ . Samples were incubated for 0, 30, or 90 min at 30 °C (without shaking), then directly mixed with an equal volume of 2  $\times$  SDS-PAGE sample buffer and heated for 5 min at 95 °C. Samples were then subjected to SDS-PAGE and western blot analysis. For analysis of the phosphorylation status of *p*-Raf1(Ser259), *p*-MEK1/2(Ser217/221), and *p*-ERK1/2(Thr202/Tyr204), samples were subjected to a standard western blotting procedure. To determine the phosphorylation status of a protein, the respective signals for the phospho-/total protein antibodies were compared.

**IP and on-bead dephosphorylation:** U2OS cells were transfected with pCMV-3FLAG-ERK1 or pEGFP(N1)-MEK1 for 48 h by using FuGene HD (Promega) following the manufacturer's instructions. Cells were then washed twice with ice-cold PBS, scraped from plates in Tris-HCl (10 mM), NaCl (100 mM), 0.1% IGEPAL, ethylenediaminetetraacetic acid (EDTA; 1 mM) and ethylene glycol-bis( $\beta$ -aminoethyl ether)-*N,N,N',N'*-tetraacetic acid (EGTA) supplemented with Protease Inhibitor Cocktail (Sigma), and PhosphoStop (Roche). Cells were subjected to mechanical lysis by five passes through a syringe needle and lysate was cleared by centrifugation (10 min,  $10^4$  rcf, 4 °C). For bait capture, anti-GFP nanobodies coupled to CNBr beads (EMBL PEPCore facility) or anti-FLAG M2 magnetic beads (Sigma) were washed twice with lysis buffer, and the lysate was subsequently incubated with beads for 2 h at 4 °C on a rotation wheel. Next, beads were washed three times with lysis buffer. Dephosphorylation was set up by incubating the bead-bound substrate with indicated amounts of PP1/Cal A for 15 min at 30 °C. Finally, beads were washed twice in buffer and protein was eluted

in SDS sample buffer by heating the beads for 5 min to 95 °C. To analyze the phosphorylation status of *p*-MEK1/2 (Ser217/221) and *p*-ERK1/2(Thr202), samples were subjected to a standard western blotting procedure.

**Analysis of MAPK dephosphorylation:** U2OS cells (at 90% confluency) were either left untreated or treated with PDP3 or PDP-Nal (10  $\mu\text{M}$ ) in Dulbecco's modified Eagle's medium (DMEM; without fetal bovine serum (FBS)) for the indicated time points. The cells were then washed twice with cold PBS, scraped in lysis buffer (20 mM Tris-HCl, pH 7.4, 137 mM NaCl, 10% glycerol (v/v), 1% NP40 (v/v), 50 mM EDTA, 1  $\times$  EDTA-free protease inhibitor cocktail (PIC), 1  $\times$  PhosStop, 10 mM  $\text{Na}_3\text{VO}_4$ , and 50 mM NaF), and centrifuged. The cleared lysate was boiled in 2  $\times$  SDS sample buffer. Equal amounts of lysate from different conditions were subjected to western blotting against MEK1/2, *p*-MEK1/2(Ser217/221), ERK1/2, *p*-ERK1/2(Thr202/Tyr204), and  $\alpha$ -tubulin antibody.

**Inhibition of PTPs:** U2OS cells were incubated with  $\text{H}_2\text{O}_2$  (1 mM) and  $\text{Na}_3\text{VO}_4$  (1 mM) in DMEM (without 10% FBS) for 30 min at 37 °C and then rinsed twice with warm PBS. The cells were treated with PDPs (10  $\mu\text{M}$ ) in DMEM (without 10% FBS) and incubated for 30 min (at 37 °C, 5%  $\text{CO}_2$ ). The cells were then washed twice with cold PBS, scraped in lysis buffer (20 mM Tris-HCl, pH 7.4, 137 mM NaCl, 10% glycerol (v/v), 1% NP-40 (v/v), 50 mM EDTA, 1  $\times$  PIC, 1  $\times$  PS, 10 mM  $\text{Na}_3\text{VO}_4$ , and 50 mM NaF), and centrifuged (13000 *g*, 4 °C for 10 min). The cleared lysate was boiled with 2  $\times$  SDS-PAGE sample buffer. Equal amounts of lysate from different conditions were subjected to western blotting against MEK1/2, *p*-MEK1/2(Ser217/221), ERK1/2, *p*-ERK1/2(Thr202/Tyr204), and  $\alpha$ -tubulin.

## Acknowledgements

This work was supported by an ERC Starting Grant (#336567) to M.K. We thank Christina Gross, BIOSS, for scientific and language editing of the manuscript.

## Conflict of Interest

The authors declare no conflict of interest.

**Keywords:** activators • amino acids • kinases • peptides • phosphorylation

- [1] M. Carrara, A. Sigurdardottir, A. Bertolotti, *Nat. Struct. Mol. Biol.* **2017**, *24*, 708–716.
- [2] M. Köhn, *J. Pept. Sci.* **2017**, *23*, 749–756.
- [3] a) T. H. Fischer, J. Eirighaus, N. Dybkova, A. Saadatmand, S. Pabel, S. Weber, Y. Wang, M. Köhn, T. Tirilomis, S. Ljubojevic, A. Renner, J. Gummert, L. S. Maier, G. Hasenfuß, A. El-Armouche, S. Sossalla, *Eur. J. Heart Fail.* **2018**, <http://doi.org/10.1002/ejhf.1297>; b) V. Sequeira, C. Maack, *Eur. J. Heart Fail.* **2018**, <http://doi.org/10.1002/ejhf.1315>.
- [4] M. Swingle, L. Ni, R. E. Honkanen, *Methods Mol. Biol.* **2007**, *365*, 23–38.
- [5] S. Fahs, P. Lujan, M. Köhn, *ACS Chem. Biol.* **2016**, *11*, 2944–2961.
- [6] J. Chatterjee, M. Beullens, R. Sukackaite, J. Qian, B. Lesage, D. J. Hart, M. Bollen, M. Köhn, *Angew. Chem. Int. Ed.* **2012**, *51*, 10054–10059; *Angew. Chem.* **2012**, *124*, 10200–10206.
- [7] G. Reither, J. Chatterjee, M. Beullens, M. Bollen, C. Schultz, M. Köhn, *Chem. Biol.* **2013**, *20*, 1179–1186.
- [8] M. M. McKay, D. K. Morrison, *Oncogene* **2007**, *26*, 3113–3121.
- [9] S. Mitsushashi, H. Shima, N. Tanuma, N. Matsuura, M. Takekawa, T. Urano, T. Kataoka, M. Ubukata, K. Kikuchi, *J. Biol. Chem.* **2003**, *278*, 82–88.

- [10] P. Rodriguez-Viciano, J. Osés-Prieto, A. Burlingame, M. Fried, F. McCormick, *Mol. Cell* **2006**, *22*, 217–230.
- [11] M. Jaumot, J. F. Hancock, *Oncogene* **2001**, *20*, 3949–3958.
- [12] H. Mischak, T. Seitz, P. Janosch, M. Eulitz, H. Steen, M. Schellerer, A. Philipp, W. Kolch, *Mol. Cell. Biol.* **1996**, *16*, 5409–5418.
- [13] P. Dent, T. Jelinek, D. K. Morrison, M. J. Weber, T. W. Sturgill, *Science* **1995**, *268*, 1902–1906.
- [14] B. Zhou, Z. X. Wang, Y. Zhao, D. L. Brautigam, Z. Y. Zhang, *J. Biol. Chem.* **2002**, *277*, 31818–31825.
- [15] X. D. Hu, Y. N. Liu, Z. Y. Zhang, Z. A. Ma, Z. W. Suo, X. Yang, *J. Neurosci.* **2015**, *35*, 13989–14001.
- [16] P. K. Wu, S. K. Hong, J. I. Park, *Mol. Cell. Biol.* **2017**, *37*, e00061-17.
- [17] I. Manfroid, J. A. Martial, M. Muller, *Mol. Endocrinol.* **2001**, *15*, 625–637.
- [18] K. Nagasaka, T. Seiki, A. Yamashita, P. Massimi, V. K. Subbaiah, M. Thomas, C. Kranjec, K. Kawana, S. Nakagawa, T. Yano, Y. Taketani, T. Fujii, S. Kozuma, L. Banks, *PLoS One* **2013**, *8*, e53752.
- [19] H. Sotoud, P. Gribbon, B. Ellinger, J. Reinshagen, P. Boknik, L. Kattner, A. El-Armouche, T. Eschenhagen, *J. Biomol. Screening* **2013**, *18*, 899–909.
- [20] J. Qian, B. Lesage, M. Beullens, A. Van Eynde, M. Bollen, *Curr. Biol.* **2011**, *21*, 766–773.
- [21] H. L. Cheng, M. J. Hsieh, J. S. Yang, C. W. Lin, K. H. Lue, K. H. Lu, S. F. Yang, *Oncotarget* **2016**, *7*, 35208–35223.
- [22] C. J. Caunt, S. M. Keyse, *FEBS J.* **2013**, *280*, 489–504.

---

Manuscript received: September 12, 2018

Accepted manuscript online: October 19, 2018

Version of record online: November 26, 2018